estec

European Space Research
and Technology Centre
Keplerlaan 1
2201 AZ Noordwijk
The Netherlands
T +31 (0)71 565 6565
F +31 (0)71 565 6040

www.esa.int

DOCUMENT

ATHENA - Telescope Reference Design and Effective Area Estimates

Prepared by Tim Oosterbroek
Reference ESA-ATHENA-ESTEC-PL-DD-0001
Issue 2
Revision 4
Date of Issue 16/02/2018
Status
Document Type TN

European Space Agency
Agence spatiale européenne

Distribution

APPROVAL

Title	
Issue 2	**Revision** 5
Author	**Date** 17/04/2018
Approved by	**Date**

CHANGE LOG

Reason for change	Issue	Revision	Date
Incorporated effective areas per row (ring) and information on calculation of vignetting for Industrial activities. Added information on Wolter-Schwartzschild configuration.	2	0	16/01/2015
Minor editorial changes	2	1	23/01/2015
Minor changes for update #2 following industry comments	2	2	05/10/2015
Revision & update to include additional rib-pitch cases and also annex on MM-layout update.	2	3	24/10/2017
Update effective area estimate based on SiC coating (replacement for B4C/Ir) and included constraints for MM-widths as function of radial position to be used by the SC Primes in re-packing the MA.	2	4	16/02/2018
Correction of step-function graph in annex defining maximum MM-widths as f(radius)	2	5	17/04/2018

CHANGE RECORD

Issue 2	**Revision** 5		
Reason for change	**Date**	**Pages**	**Paragraph(s)**

Table of contents:

1.1 Applicable Documents

[AD01] Space engineering: System engineering general requirements, ECSS-E-ST-10C, Issue 3.0, 06/03/2009.

1.2 Reference Documents

[RD01] IXO Silicon Pore Optics Mirror Modules performance specifications and interface requirements – Issue 2.2 – 15 Feb 2011.

[RD02] Assumptions for estimating the effective area of the IXO telescope – Issue 1.0 – 28 January 2010 (SRE-PA/2010.010/NR).

[RD03] Reference IXO telescope geometric design and effective area estimates - Issue 1.0 – 3 February 2010 (SRE-PA/2010.011/).

[RD04] Reference IXO telescope geometric design and effective area estimates for a reduced outer radius – Issue 1.0 – 31 March 2010 (SRE-PA/2010.021).

[RD05] IXO reference design and effective area estimates using dual Stacks – Issue 1.0 – 17 February 2011 (SRE-PA/2011.011).

[RD06] ATHENA telescope reference design and effective area estimates – Issue 2.0 – 15 June 2011 (SRE-PA/2011.049).

[RD07] ATHENA telescope reference design and effective area estimates for F=12m – Issue 1.0 – 14 October 2011 (SRE-PA/2011.096).

[RD08] ATHENA - SC<>MM ICD, ESA-ATHENA-ESTEC-SYS-IF-0004, Issue 1.1, 01/08/2017.

1 INTRODUCTION & SCOPE

This document is an instantiation of the Analysis Report standard (Annex Q of [AD01]), as part of the Mission DJF. It presents a reference design for the ATHENA Mirror Assembly (MA) and is intended, along with the SC<>MM ICD [RD08] which is consistent with it, to provide a starting point for the SC Primes when considering their MA design. A MA reference design is provided for the 15-row MA; an additional 16th row is also included. It is a reference only and it is expected that the Primes depart from the reference MM-layout presented here as they mature their MA designs. **Guidelines for this departure are provided.**

This document contains the following spreadsheets:

- MM_area_tool_2018.xls
- mm_2018.xls
- Pos_2018.xls.

2 REFERENCE MA DESIGN

2.1 MM - Design

The MM designs used in this model are consistent with latest evolution of the optics technology development:

- As in [RD05], [RD06] and [RD07], "dual-stacks" are adopted, i.e. in one MM 2 sets of P-S stacks are mounted together in a common bracket, separated by a distance equivalent to the typical plate-to-plate separation (< 1 mm).
- Each XOU stack has 35 plates of which 34 are reflective and contributing to the A_{eff}, while the remaining plate (on the inside of each stack) is non-reflecting and acts as a stray-light baffle. One MM therefore has total of 140 plates, 136 of which are reflecting.
- Each stack consists of either Primary (P) parabolic or Secondary (S) hyperbolic plates. Each plate has a thickness of 0.170 mm, and a pore height of 0.605 mm. The ribs between the plates have a width of 0.17 mm and a conservative pitch of 1 mm[1].
- The two pairs of stacks within one mirror module are separated by the space normally reserved for one plate (0.775 mm). Such a separation distance is presently a working assumption that will need to be confirmed during the planned technology development activities.
- The reflective surfaces are coated with a 10 nm SiC coating on top of 10 nm Iridium. Note that this assumption has changed with respect to the previous versions, since the B_4C coating is not a viable option anymore (it does not survive a standard cleaning process – RCA Standard Clean I, used in the processing of the SPO plates). The thickness of the SiC is optimized using the ATHENA geometry for an energy of 1 keV. The actual optimized value is 9.9 nm, but 10 nm is used for simplicity.
- All MMs have a Focal Length (FL) of 12 m.

In order to simplify the A_{eff} estimate, the following approximations are made:

- The conical approximation is used for the P-S plates; this differs from the values derived from a true Wolter I geometry at (at most) μm level. The radii have been calculated using the optimal plate length, for the 35th reflecting (approximately middle) plate in a mirror module, (given by $l(r) = h_0/\tan\alpha$, where h_0 is the pore height (0.605 mm) and α the grazing angle given by $\tan 4\alpha = r/F$, with F the focal length (12

[1] In the ATHENA proposal a rib pitch of 3 mm is proposed, to increase the A_{eff} and Grasp (flatten the vignetting curve). The spreadsheet 'MM_area_tool_2018' includes entries for rib pitches of 1., 2.,, and 2.3 mm to show the effect (purely geometric and so proportionally the same at all energies) of increasing the rib-pitch. Some increase in rib-pitch can be anticipated, and is currently being explored in the technology developments.

m) and r the radius). In the conical approximation the angle of the parabolic plate with the optical axis is α, while the angle of hyperbolic plate with the optical axis is 3α.

- It is assumed that the two pairs of stacks in each MM are identical, disregarding any geometrical difference in circumferential length. In reality each pair of stacks will have a slightly different length. Inclusion of such a difference would only impact at ~1% level the EA calculations.

2.1.1 MM - Vignetting

Note: The A_{eff} estimates in this document do not include the effect of vignetting – however a brief description is provided here of vignetting effects at MM-level which provides a starting-point for its' evaluation.

Vignetting occurs when there is misalignment between the optical axis of a MM and the LoS, resulting in a reduction of A_{eff}. Two directions (terms) can be distinguished: perpendicular to the reflecting surface (rotation around the X-axis, see Figure 1; note that the MM coordinate frame is different from the MA reference frame) and a rotation around the Y-axis.

Vignetting at MM-level can be modelled by a triangular function (see Figure 2); this triangular shape assumes perfect internal alignment of the MMs and can therefore be considered as conservative in terms of vignetting. Total vignetting is the product of the two terms (which ignores small "cross-terms"). In Table 1 the half-zero-widths are provided for the two rotation directions, for three different rib pitches. If the value is larger than this half-zero-width the MM is essentially 'blind' and no photons will be focused on the focal plane. For an individual MM the misalignment angle needs to be decomposed into rotations around the X- and Y-axes and vignetting in the two directions can then be calculated.

MA-level vignetting can therefore be evaluated by considering r-x, r-y rotations incurred at MM-level with respect to a global MA-coordinate system.

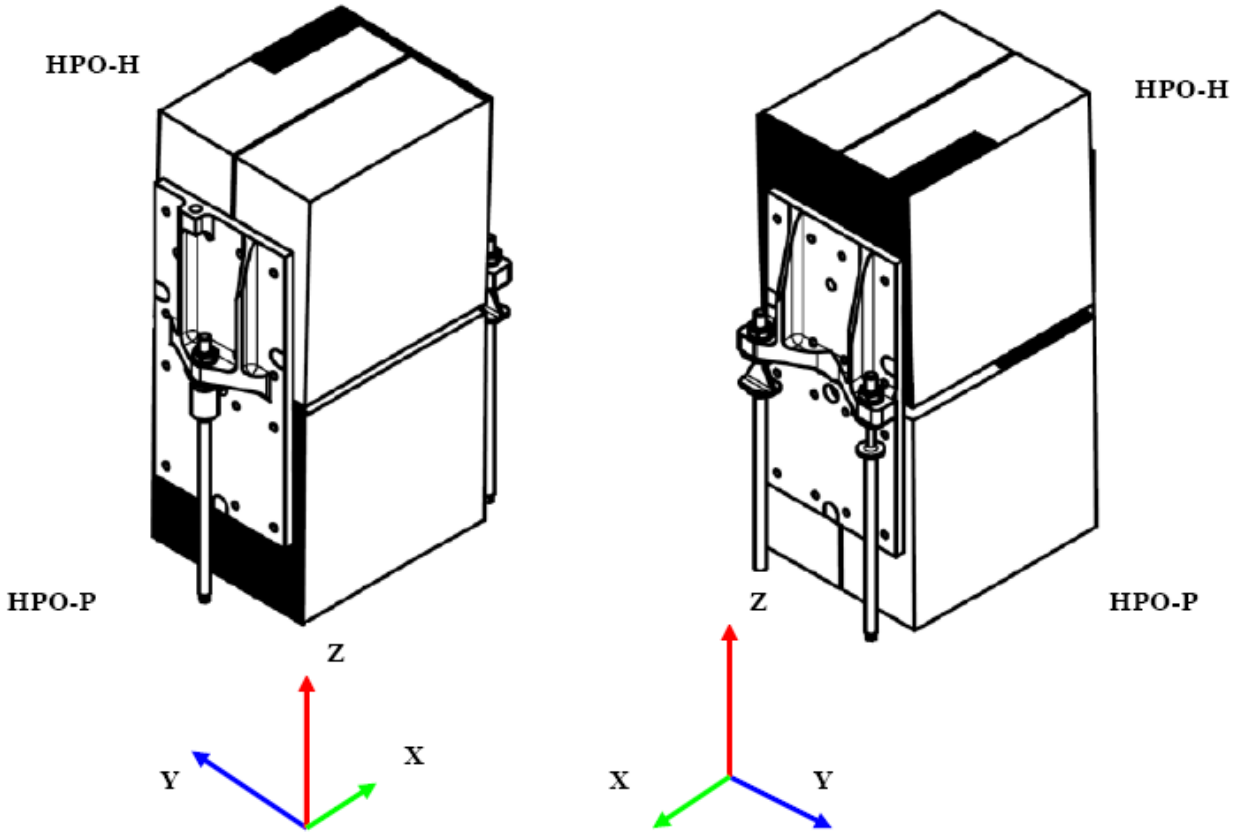

Figure 1: MM reference frame, seen from two sides. The Y-coordinate is radially outward in the telescope configuration, the Z-axis points towards the focal plane

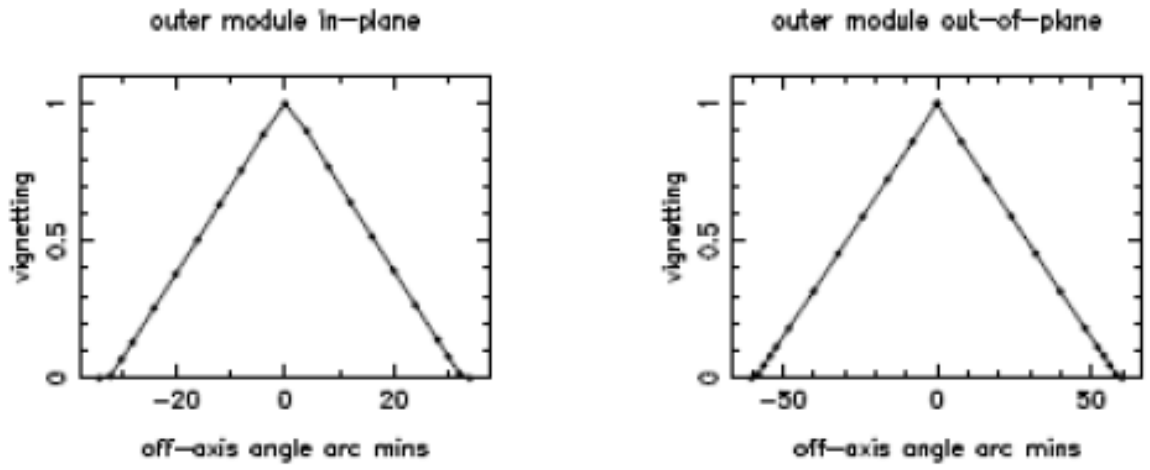

Figure 2: Example of the shape of the vignetting function for a MM

Row	HZW_X (deg)	HZW_Y (deg)		
		1mm	2mm	3mm
1	0.1864	0.25572	0.5638	0.87185
2	0.22348	0.3066	0.67597	1.04528
3	0.26055	0.35746	0.78809	1.21864
4	0.29761	0.40831	0.90018	1.39192
5	0.33466	0.45913	1.01222	1.56511
6	0.37169	0.50993	1.1242	1.7382
7	0.4087	0.56071	1.23611	1.91117
8	0.44568	0.61146	1.34796	2.08401
9	0.48265	0.66218	1.45973	2.25671
10	0.51958	0.71286	1.57141	2.42926
11	0.55649	0.7635	1.683	2.60164
12	0.59337	0.81411	1.7945	2.77384
13	0.63022	0.86468	1.9059	2.94586
14	0.66704	0.9152	2.01718	3.11768
15	0.70382	0.96567	2.12836	3.28929
16	0.74056	1.0161	2.23941	3.46067
17	0.77727	1.06647	2.35033	3.63183
18	0.81393	1.11679	2.46112	3.80274
19	0.85055	1.16705	2.57177	3.97339
20	0.88713	1.21725	2.68227	4.14378

Table 1: Vignetting half-zero-widths for two directions and three different rib pitches - the subscript X refers to a rotation about the X-axis, while the subscript Y refers to a rotation about the Y-axis

2.2 MM - Layout

Note: See spreadsheets (mm_2018.xls and pos_2018.xls).

The MM-layout is similar to those presented in [RD03], [RD04], [RD05] which presented designs for IXO, and [RD06], [RD07] which presented designs for ATHENA_L1. The MM-layout for one petal is shown in Figure 4. The lay-out is identical to the previous version of this note. It was decided not to change the lay-out of the MMs at this time. The main features are as follows:

- The MMs will be arranged in the so-called Wolter-Schwartzschild configuration which improves the off-axis PSF performance. In this geometry the mid-planes of the MMs are arranged on a spherical plane (see Figure 3). The sphere has a radius equal to the focal length of the telescope. The displacement of the mid-points of the MMs parallel to the optical axis is therefore given by $\sqrt{(F^2-R^2)}$, where F is the focal length, and R the radius of the MM.

- The spacing between the MMs (Si-Si distance) is a constant azimuthal separation of 16.8 mm and a constant radial separation of 7 mm (note: these distances will be

derived by Primes for their own MAM design, and may not be constant). The separations are identical to the values used in [RD04] and later. It should be noted that meeting this spacing over the whole of the MA poses challenges to the structural design of the MA, and the obtained A_{eff} estimates will rely sensitively on this spacing. **Prime departures from this spacing should be accompanied by a preliminary A_{eff} estimate tool (can be derived from the tool attached to this document) to evaluate the A_{eff} changes associated with any changes.**

- The MA consists of 6 identical 'petals' or sextants, and so has 6 degrees of rotational symmetry.

- The minimum radius for a MM is 0.25 m, driven by: Minimization of technology risk (limiting the radius of primary curvature of the plates); leaving a 50 cm Ø space at the MA centre for accommodation of metrology units.

- The following constraints on MM-width (arc-length) are imposed[2]:
    - A maximum width of 6 cm for radii below 0.50 m (rows 1→4)
    - A maximum width of 10 cm for radii larger than 0.50 m (rows 5→20).

  For a particular row, packing the MMs then simply targets the lowest integer number of MMs that fits a sextant, while meeting these constraints. These are initial assumptions and are currently being revisited to better understand the maximum allowable width for a particular radius, and also the overall impact on re-packing the MA (**see Annex: MM - Layout Re-packing Exercise, which also specifies the current constraints on MM-width as a function of radial position that can be considered by the Primes when departing from the reference design**).

Spreadsheet 'mm_2018.xls' details the length of the parabolic and hyperbolic part of each plate in each row (L), the radius at the point closest to the focal plane (R_H), the radius at the mid-plane (R_M), the radius at the point furthest from the focal plane (R_P) and the width (W) of the plate. All units are in m. The length of the plates has been derived from the optimal length for the 35th reflective plate (approximately middle plate) in a MM.

Spreadsheet 'pos_2018.xls' defines the position of the mid-point of the parabolic-hyperbolic join of the 35th reflecting plate in a coordinate frame with the optical axis at (0,0). For each row this position is specified for each MM. The choice for tabulating the position of the 35th reflective plate (out of 68 reflecting plates and 70 in total) is driven by the fact that the number of plates is even and therefore no middle plate can be assigned. It should be noted that therefore this position does not exactly correspond to the mid-point of the MM.

[2] This is the main difference with respect to previous designs where the MM-width constraint was the same at each radius.

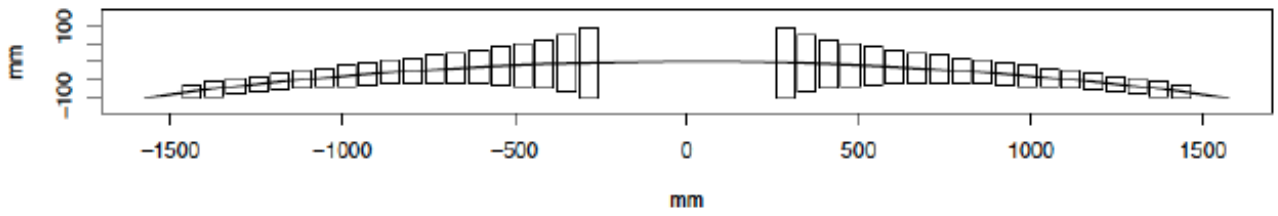

Figure 3: Illustration of the curved principal plane of the Wolter-Schwartzschild configuration. The focal plane is at the bottom

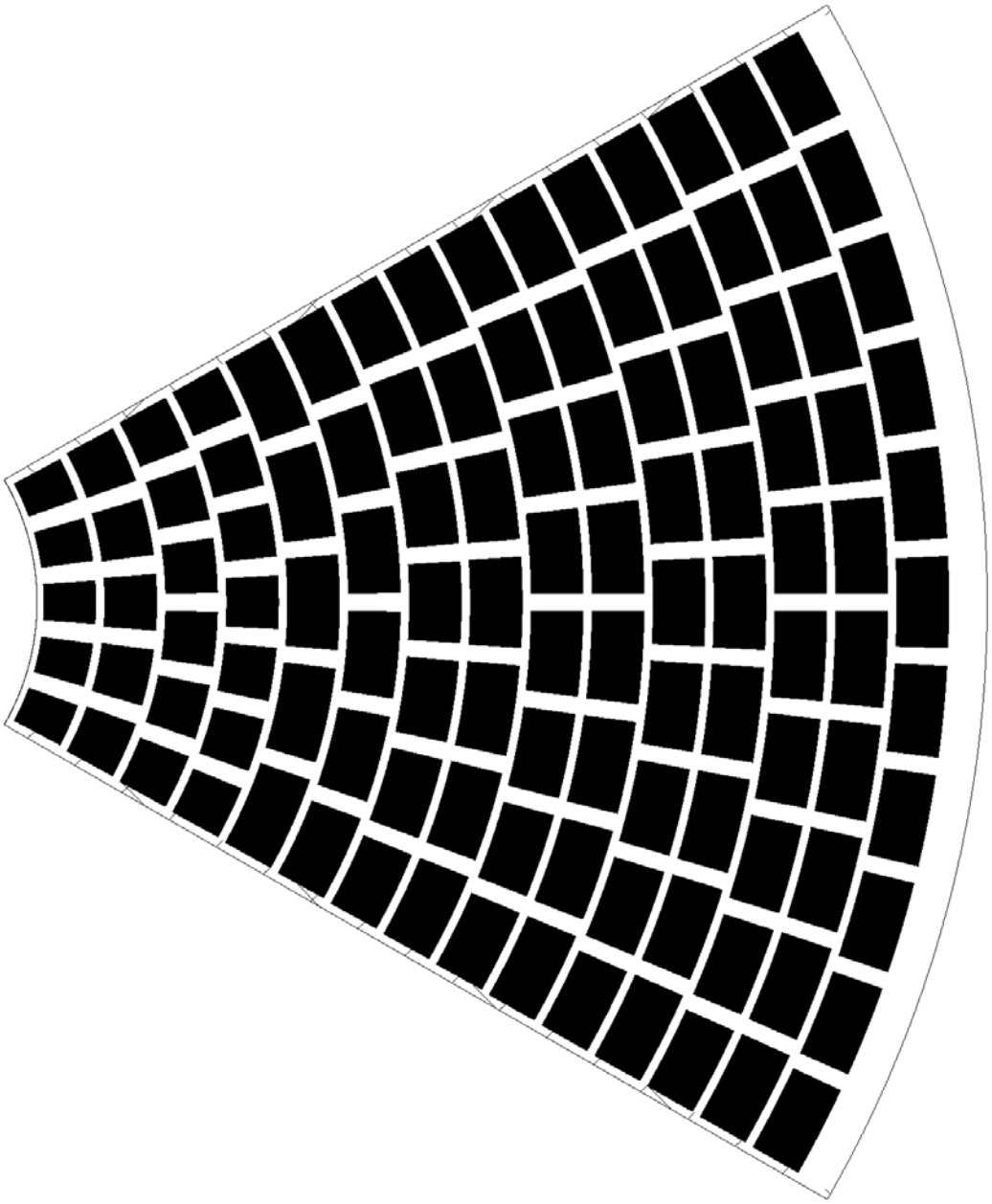

Figure 4: Schematic MM-layout in one ‘petal’ (15 rows)

3 EFFECTIVE AREA

Note: see spreadsheet 'MM_area_tool.xls' *which calculates* A_{eff} *at 1 & 7 keV for the reference MM-layout, and allows toggling of FL & row# and where additional degradation factors (on top of the already included 10% loss) can be included as well. The tool also presents the impact of 1, 2 & 2.3 mm rib-pitch, which is a geometric effect resulting in a constant factor applied to* A_{eff} *at all energies, though note the reference value remains 1 mm.*

The A_{eff} of the MA is calculated using Henke tables for the assumed coating, without taking into account effects like contamination and assumes perfectly smooth surfaces (i.e. no micro roughness). A 10% margin loss is applied to the values presented throughout this document. This value is detailed in [RD02] and consists of, amongst others, of alignment losses and losses due to particulate contamination. Net A_{eff} (including the 10% loss) is summarised in Table 1, and Table 3 summarises the MA layout. Figure 5, Figure 6 show A_{eff} estimate curves for the 20-row and 15-row MA designs respectively.

Max. Width	A_{eff} @ 1 kev [m^2]	A_{eff} @ 7 kev [m^2]	# MM	# rows
6/10 cm	1.36	0.152	678	15

Table 2: Reference MA A_{eff} at two reference energies (including 10% loss) for the 15-row design. A 16th row is also included.

Row	Width (mm)	Length (mm)	Number of MMs	Middle radius (m)	A_{eff} p. row @ 1 keV [m^2]	A_{eff} p. row @ 7 keV [m^2]
1	37.096	101.504	30	0.286	0.0321981	0.027232694
2	50.158	83.388	30	0.348	0.0429483	0.02859941
3	49.838	70.762	36	0.411	0.0505464	0.025687212
4	49.613	61.46	42	0.473	0.0579159	0.028135352
5	89.363	54.321	30	0.535	0.0733565	0.028108829
6	82.476	48.671	36	0.597	0.0801211	0.012131376
7	77.571	44.087	42	0.659	0.0866314	0.001072647
8	86.892	40.294	42	0.722	0.0955172	8.78665E-06
9	82.053	37.104	48	0.784	0.101432	0.000128045
10	90.205	34.383	48	0.846	0.109602	0.000350511
11	85.538	32.036	54	0.908	0.114846	0.000161755
12	92.782	29.99	54	0.97	0.122205	1.02409E-05
13	88.326	28.191	60	1.032	0.126675	1.12726E-07
14	94.845	26.597	60	1.095	0.133101	2.50773E-06
15	90.608	25.175	66(Σ678)	1.157	0.136664	9.87596E-06
16	87.079	23.898	72	1.219	0.139737	1.70345E-05

Table 3: Summary table of the telescope design for 15 rows plus an additional 16th row.

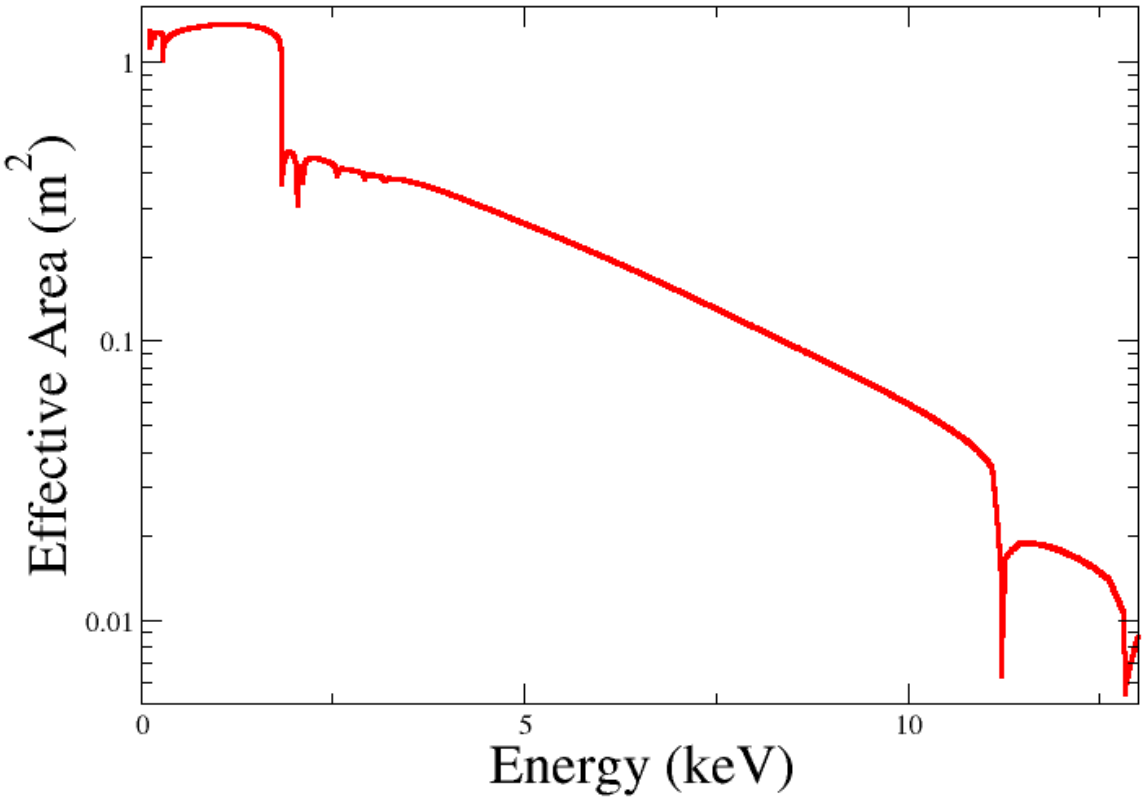

Figure 5: A_{eff} curves for the 15-row MM-layout (logarithmic abscissa; linear ordinate); 10% losses are included

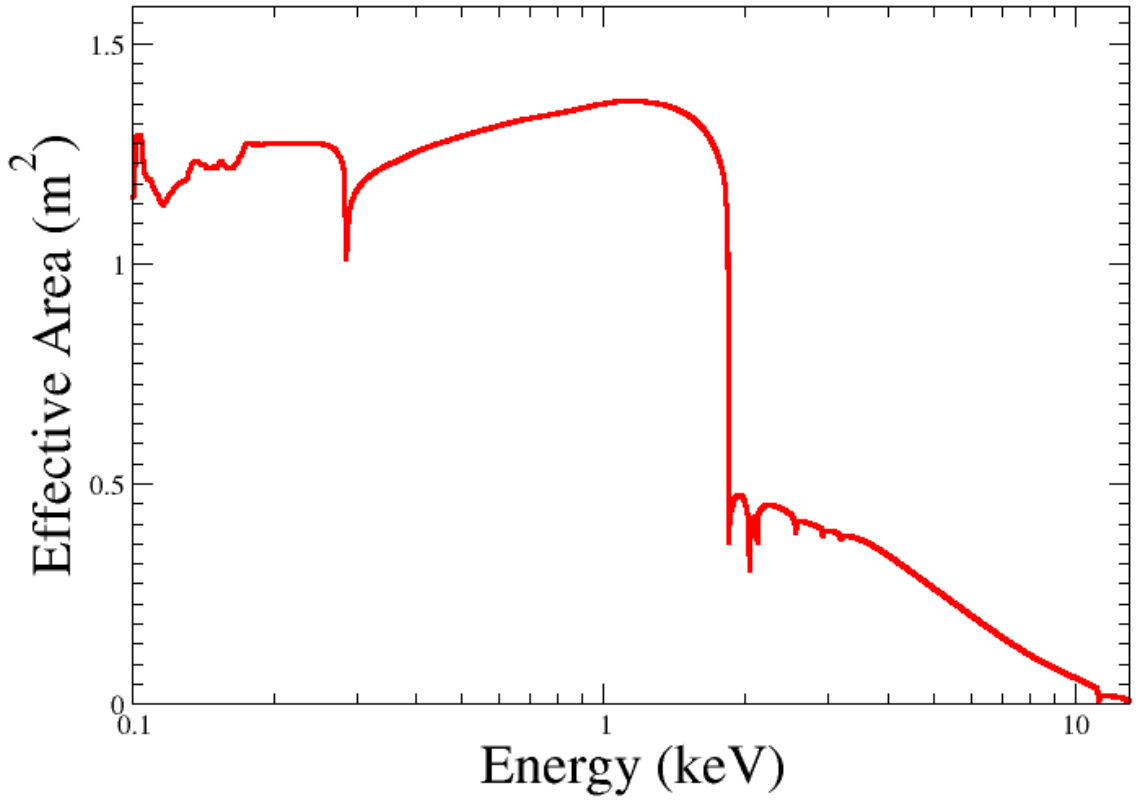

Figure 6: A_{eff} curves for the 15-row MM-layout (linear abscissa; logarithmic ordinate); 10% losses are included

	2 mm rib pitch	2.3 mm rib pitch
Rib pitch area factor	1.1024	1.1158

Table 4: Correction factors for effective areas for rib pitches different from the 1mm baseline rib pitch. Since rib pitch only affects the geometrical area this factor is independent of energy.

ANNEX: MM - LAYOUT RE-PACKING EXERCISE

The layout of the MMs in the MA is being investigated, with a view to updating the reference layout in time for the start of Phase B1 – the motivation is to reduce the #MMs, for both performance and cost reasons; less MMs (larger arc-length per MM) implies:

1. Better packing density and an associated increase in the A_{eff}
2. Diminution of longitudinal edge effects (TBC) leading to improved HEW
3. Reduced production costs (1st order scaled with #MMs).

3.1 Spoke # & Re-packing – General Considerations

Note: The attached spreadsheet 'MM - layout' allows a rough exploration of the impact of re-packing the MA aperture *with MMs – it is not intended to replace ('MM_area_tool.xls') for calculating the Effective Area.*

Preliminary MAM structural analysis by the Primes and ESA has indicated that keeping the MA as stiff as possible is desirable in order to minimise the strain energy that is stored in the MS during launch, constraining high loads corresponding to drum-modes, at the MA centre. There was accordingly a discussion about increasing the # spokes from 6→12 to improve the stiffness of the MA, and also to reduce inter-spoke 1g effects that are present during vertical orientation ground-phases (long-beam x-ray facility).

The reference MM-layout presented in this document imposes folding-symmetry as a constraint, but does not consider any dimensions for the spokes themselves. This is unrealistic as indeed at least 6-spokes of non-zero dimension are necessary to:

- Provide stiffness to the MS (load-reduction during launch)
- Provide harness routing for the TCS and metrology pack at the MA centre.

A preliminary analysis using the 'MM – layout' tool, which includes spoke dimensions, is used here to explore the impact of varying the spoke # and widths on the #MMs and overall MM area. The tool takes as input the updated reference 'design 0' as per §2 and, in response to a user-defined inter-MM spacing (δ_{circ}) and spoke width (Δ_{circ}), both assumed constant for all rows, re-packs the MA aperture while adhering to user-defined constraints on MM-width as a function of row. The tool assumes that the radial spacing (δ_{rad}) between MM rows is a constant 8 mm.

For a range of spoke # and widths (Δ_{circ}), and allowed % violation of the original constraints on MM arc-length (60 mm rows 1→4, 100 mm row 5 onwards), the impact on #MMs and % change in overall area (a proxy for the change in 1 keV A_{eff}) can be seen in the following figures. The following conclusions can be drawn:

1. The area loss is mild for 6-spoke cases, increasing with assumed spoke-width: Indeed the null spoke-dimension case actually shows a small increase in A_{eff} can be achieved

with the re-packing exercise as the width-constraint is relaxed (first set of green columns in Figure 8); the 10 mm spoke-dimension case is ~neutral. For larger spoke-dimensions the A_{eff} loss is ~few %. Generally, it can be stated that the negative impact of introducing a spoke dimension is largely offset by the reduction of # MM enabled by width-constraint violations (less gapping).

2. However, the switch from 6→12 spokes (Figure 8: red columns) is punitive in terms of overall MM-area, and significantly reduces the opportunity to reduce MM# by re-packing (Figure 7: red columns); a consequence of the increased symmetry constraint imposed. Note that the area associated with high energies is worse affected, and this can lead to a ~15% reduction for larger values of Δ_{circ} (not shown in the figures, but included approximately in the spreadsheet).

3. As the spoke-width increases, the inter-spoke arc decreases, and there is more opportunity to fill the row with a lower integer number of MMs as the width-constraints are relaxed (decrease in columns in Figure 7 with Δ_{circ}), thereby driving the #MM down.

4. As the allowed violation of MM arc-length increases, there is more opportunity to fill the row with a lower integer number of MMs (decrease in columns in Figure 7 for a particular Δ_{circ} case), thereby driving the #MM down. This effect is cumulative with [3].

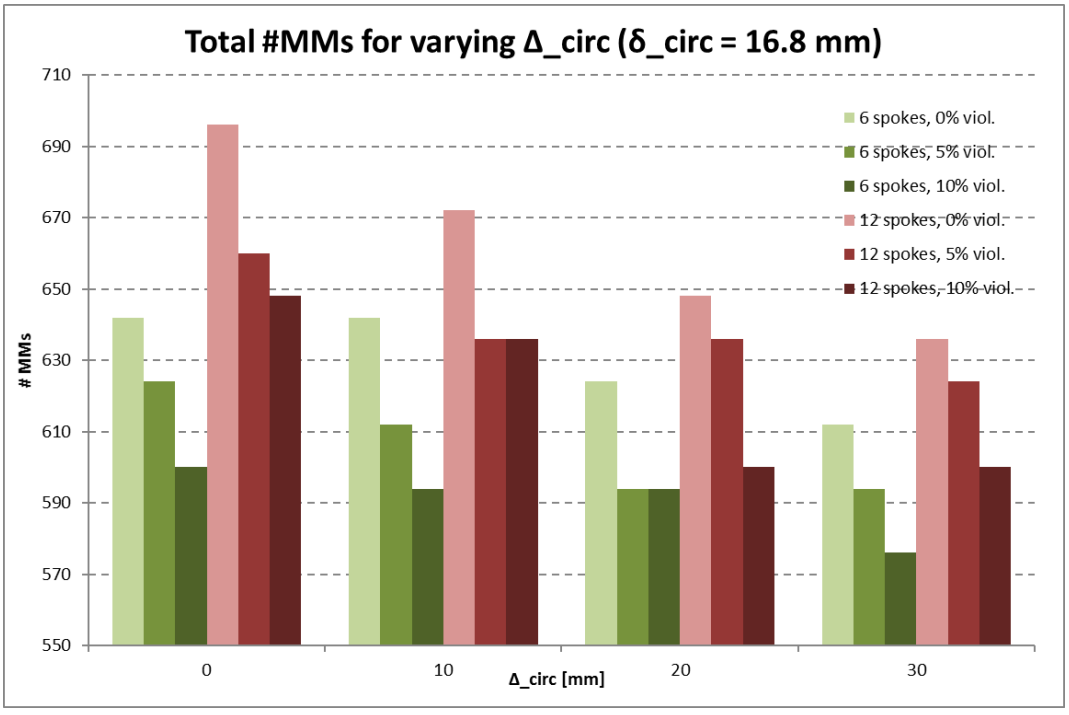

Figure 7: Total #MMs for varying spoke dimension Δ_{circ} (δ_{circ} = 16.8 mm)

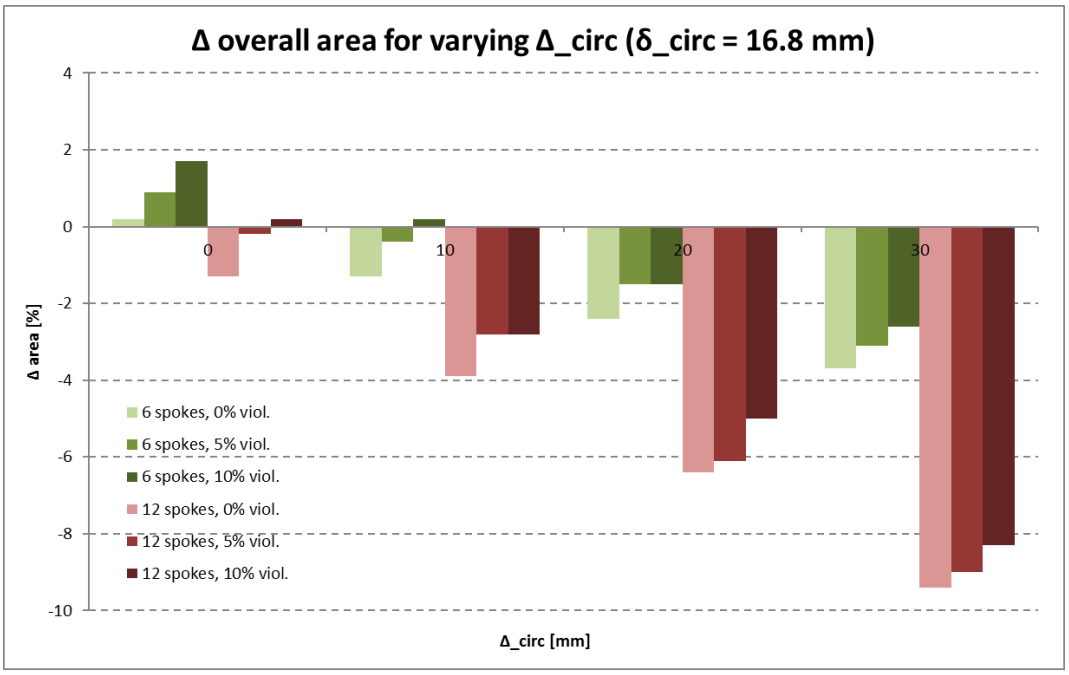

Figure 8: Total MM area (proxy for overall 1 keV A_{eff}) for varying spoke dimension Δ_{circ} (δ_{circ} = 16.8 mm)

Given these results, and given also that:

- Harness routing has been demonstrated by the SC Primes for a 6-spoke, 20-row mirror
- A reduction to 15 rows will by itself contribute ~factor 2.5 to increasing the stiffness of the MA
- We may take a 6-shot Glucksrad approach to testing and calibrating the MA in XRCF, which will reduce a lot the 1g impact (illumination with circumferential ribs aligned with g)
- Retaining a 6-spoke design will allow a very significant reduction in the total #MM count, saving some millions of Euros.

The conclusion is that pursuing a 12-spoke design is not attractive.

3.2 SC Prime Re-packing: MM-Width Constraints

Note: optimally a smooth function of maximum MM-width as a function of radial position would be provided; however, this was not a tenable exercise and so the discussion with cosine on allowable widths was restricted to a few design cases as presented hereafter. The constraints defined in this section are a starting point from this discussion, and allows some design freedom to the Primes to optimise the MA (lower #MM).

The spacings from the Prime MA layouts at the time of dMCR have been aggregated and then a realistic mid-point for inter-MM spacing (δ_{circ}) and spoke width (Δ_{circ}) applied to generate updated MM-layouts using the Reference Telescope tool. The following values were assumed, constant at all radii:

- δ_{rad} (MM<>MM radial spacing): 8 mm
- δ_{circ} (MM<>MM azimuthal spacing): 17 mm
- Δ_{circ} (spoke width): 8 mm.

Table 5 shows the resulting updated MM-layout (i.e. applying the original constraints on MM-width) as 'Design 0'. Options which progressively violate the MM-width constraints selectively are then presented as Designs A-, A, B & C. Figure 9 shoes the resulting MM-layout per sextant for the various options, and Table 6 shows the impact on A_{eff} for an assumed 1 mm rib-pitch and including a 10% loss factor.

All widths in Table 5 have been evaluated as feasible by cosine, and therefore the constraints applied to MM-width limitations that can be considered by the Primes when departing from the reference design can be taken as the following:

- **Radial positions for rows 1→4: 60 mm or max. width in** Table 5.
- **Radial positions for rows 5→15: 100 mm or max. width in** Table 5.

Applying these rules results in a step-function of allowable widths with radial position (the radial position used in 'Rm' as defined in §2.2) as shown in Figure 10. This is also provided in worksheet 'mm_2018.xls'.

			Design 0		Design A-		Design A		Design B		Design C	
	L1 (mm)	L2 (mm)	W (mm)	# MM	W (mm)	#MM	W (mm)	#MM	W (mm)	#MM	W (mm)	#MM
Row 1	111.935	101.619	48,881611	4	48.881611	4	48,881611	4	48,881611	4	48,881611	4
Row 2	89.825	83.060	49,064041	5	65.686806	4	49,064041	5	49,064041	5	49,064041	5
Row 3	75.012	70.236	49,191879	6	62.485783	5	62,485783	5	62,485783	5	62,485783	5
Row 4	64.396	60.846	49,28632	7	60.366558	6	60,366558	6	75,910255	5	75,910255	5
Row 5	56.415	53.672	89,336403	5	89.336403	5	89,336403	5	89,336403	5	89,336403	5
Row 6	50.196	48.014	82,719566	6	82.719566	6	102,763687	5	102,763687	5	102,763687	5
Row 7	45.215	43.438	93,897186	6	93.897186	6	93,897186	6	93,897186	6	116,191788	5
Row 8	41.135	39.659	87,582397	7	105.075249	6	105,075249	6	105,075249	6	105,075249	6
Row 9	37.732	36.487	97,157471	7	116.253677	6	116,253677	6	116,253677	6	116,253677	6
Row 10	34.851	33.787	91,229881	8	106.732758	7	106,732758	7	106,732758	7	106,732758	7
Row 11	32.380	31.460	99,604759	8	116.308220	7	116,30822	7	116,30822	7	116,30822	7
Row 12	30.238	29.435	94,067406	9	107.979767	8	107,979767	8	107,979767	8	107,979767	8
Row 13	28.363	27.656	89,641312	10	101.509720	9	116,354866	8	116,354866	8	116,354866	8
Row 14	26.708	26.081	96,338028	10	108.952095	9	108,952095	9	108,952095	9	108,952095	9
Row 15	25.237	24.677	92,109238	11	116.394539	9	116,394539	9	116,394539	9	116,394539	9

Table 5: Per-row summary (L1: Primary stack length, L2: Secondary stack length, W: MM width, #MM: #MM per sextant)

	# MM	A_{eff} @ 1 keV	A_{eff} @ 6 keV
Design 0	654	1.386	0.221
Design A-	582	1.417	0.228
Design A	576	1.420	0.226
Design B	570	1.422	0.228
Design C	564	1.425	0.229

Table 6: Summary of design case #MMs, and A_{eff} at 1 and 6 keV

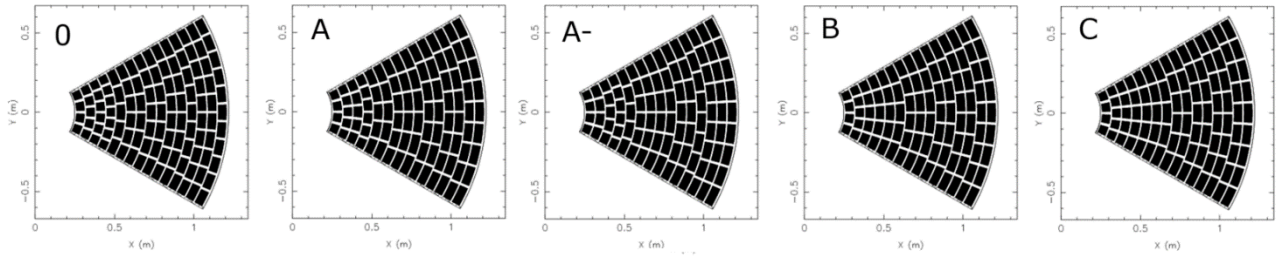

Figure 9: MM-layout cases as per the previous tables

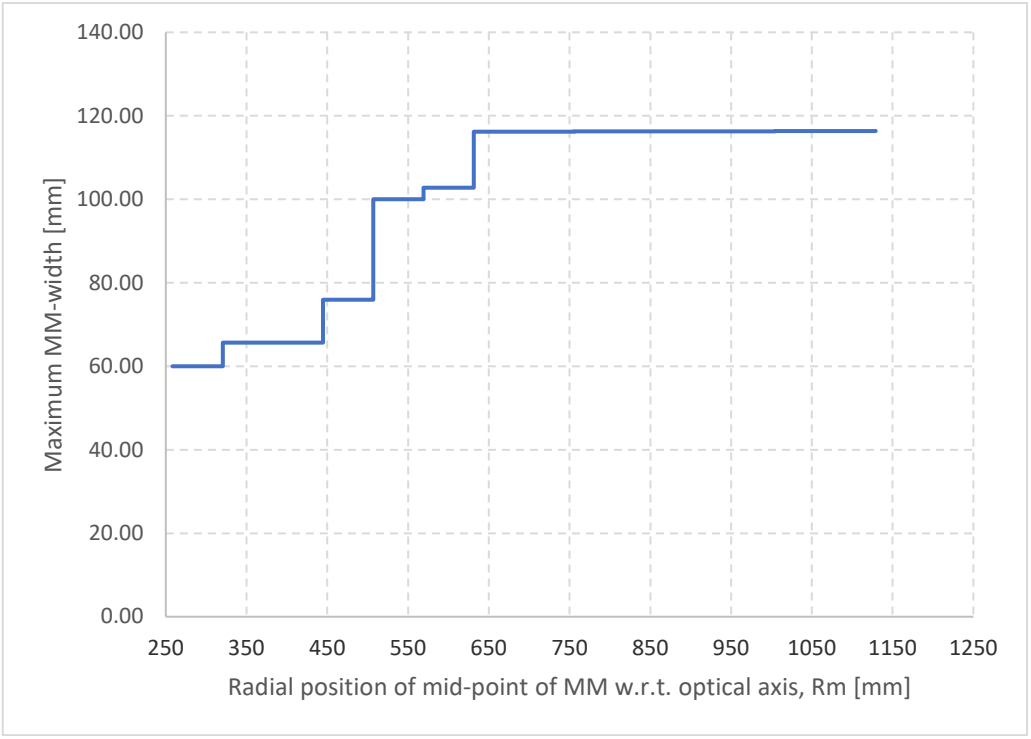

Figure 10: Allowable MM-width as a function of radial position w.r.t. the optical axis